JOURNAL OF BACTERIOLOGY, Dec. 1975, p. 1529-1544
Vol. 124, No. 3

Printed in U.S.A.

Surface Arrays on the Cell Wall of *Spirillum metamorphum*

T. J. BEVERIDGE* AND R. G. E. MURRAY

Department of Bacteriology and Immunology, University of Western Ontario, London, Ontario, Canada.

Received for publication 10 September 1975

A complex and easily disrupted arrangement of macromolecules was present on the outer (lipopolysaccharide) membrane of the cell wall of *Spirillum metamorphum*. Separation of the arrays from the cell and spontaneous reassembly into regularly structured complexes usually occurred during preparation for electron microscopy. Freeze etchings, thin sections, and optical diffraction analysis of negatively stained fragments indicated that they consisted of two sets of a thin layer which was studied with 3-nm particles arranged in a loose (OL). The OSL consisted of a hexagonal arrangement of 8-nm disks and the OL of a thin layer which was studied with 3-nm particles arranged in a loose rectangular manner. The OSL of reassembled fragments displayed numerous broken delta-linkers between units and a center-to-center spacing of half the expected distance, which suggests that an interdigitation of two OSL arrays had occurred. These observations combined with freeze etchings and thin sections of whole cells suggested a possible reassembly mechanism. The normal surface arrangement of these layers on cells was thought to consist of the OL overlying one set of OSL which was loosely adherent to a thin amorphous backing layer.

Spirillum serpens strain VHA, *S. putridiconchylium*, *S. metamorphum*, and *Spirillum* "Ordal" are representative of freshwater spirilla and, with the exception of the Ordal strain, are included by Hylemon et al. in the proposed genus *Aquaspirillum* (11), for which *S. serpens* (Muller) is the type species. All of these provide examples of complex macromolecular arrangements discernible by electron microscopy: (i) the outer (lipopolysaccharide) membrane (OM) of the cell wall of *S. serpens* VHA is covered by a single layer of hexagonally packed and Y-linked units (5, 14); (ii) cells of *S. putridiconchylium* are covered by two superficial layers—an outer linear array of small particles which is intimately associated and in contact with an inner tetragonal array of larger units (3); (iii) the Ordal strain (probably a variant of *S. anulus*) is unusual in having a complex of five superficial layers (T. Beveridge and R. G. E. Murray, submitted for publication), three of which show regular structure (a hexagonally packed and delta-linked layer, a close-packed, tetragonally arrayed layer, and a less distinct linearly arrayed layer); (iv) *S. metamorphum* has provided a novel type of multilayered superficial wall structure and difficulties in structural analysis, which we will describe in this paper.

The surface layers of *S. metamorphum* tended to fragment and reassemble, during growth in liquid media, as highly complex sheets of regular structure. Since these sheets proved readily available and suitable for high resolution characterization, they were studied first. This information was then applied to the interpretation of the normal appearance of the superficial structure of the cell surface.

MATERIALS AND METHODS

Organism. *S. metamorphum* (now obtainable as ATCC 15280) was received from N. R. Krieg (Department of Biology, Virginia Polytechnic Institute, Blacksburg, Va.).

Cultivation. The organism was routinely maintained on peptone-succinic acid-salts-yeast extract (PSSY) semisolid medium (3). For electron microscopy studies, the cells were grown in 50 ml of PSSY broth at 30 C on a rotary shaker until an early, mid, or late logarithmic growth phase (mean generation time, 41.7 min). Calcium (1 mM $CaCl_2$) was routinely added to the medium in an attempt to maintain the integrity of the superficial layers.

Preparation for electron microscopy. (i) Negative staining technique. Samples of the cell suspension or superficial wall fragments were mixed either 1:2 with 1% phosphotungstic acid (pH 7.0), 1:2 with 2% uranyl oxalate (pH 7.0), 1:2 with 0.1 M sodium zirconyl glycollate (pH 7.0), or 1:2 with 1% ammonium molybdate (pH 7.0), all of which contained 1 mM $CaCl_2$, and were processed as previously outlined (3). The cells were separated from the reassembled regular structured pieces by centrifugation at 3,000 × *g* for 15 min, and the reassemblies were collected by centrifugation at 18,000 × *g* for 30 min.

(ii) Fixing, embedding, and sectioning

technique. Prefixation of either early or mid-logarithmic cells was accomplished in a mixture of 4% glutaraldehyde-5% acrolein in 0.2 M cacodylic acid buffer (pH 7.2) containing 500 μg of ruthenium red for 15 min at 23 C. Fixation was attained in a solution similar to that used for prefixation except 2% tannic acid was added. Cells were fixed for 1 h at 23 C. The tannic acid and cacodylic acid were obtained from the Fisher Scientific Co., Fair Lawn, N. J., the acrolein from the Eastman Kodak Co., Rochester, N. Y., and the glutaraldehyde (as an 8% aqueous solution) and the ruthenium red from Polysciences Inc., Warrington, Pa. The postfixation and staining procedures were as previously described (3).

Two embedding media were used, Vestopal W (Martin Jaeger, Vésenaz, Geneva, Switzerland) and water-miscible Durcupan (Fluka AG, Buchs SG, Switzerland), and these were processed as previously described (3).

All embeddings were cut on a Reichert model OMU2 ultramicrotome with glass knives, and sections were collected on carbon-Formvar-coated 200-mesh copper grids. The sections were stained with 1% uranyl acetate and lead citrate (16) before viewing in the electron microscope.

(iii) Freeze-etching technique. Samples for freeze etching were processed according to Buckmire and Murray (5) and stored in liquid nitrogen for no longer than 48 h. Etching times varied between 30 and 90 s. Cryogens were not utilized, since both surface structure damage and inappropriate cleavage resulted. The apparatus used was a Balzers model BA510M (Balzers AG, Liechtenstein).

Electron microscopy. A Philips EM-300 electron microscope operating at 60 kV was used throughout. Micrographs were taken on Kodak fine-grain positive film. Negatively stained catalase crystals (Worthington Biochemicals Corp., Freehold, N. J.) were used as a calibration standard (7).

Optical diffraction and reconstruction. A Polaron optical diffractometer (Polaron Instruments Ltd., London, England) and a Spectra Physics, model 132, helium-neon laser, were used as previously described (3).

Indexing of the reflections in optical transform. A system of indexing, known as the Miller system, has been universally adopted to define the spatial orientation of molecules in a crystal face (17). Unfortunately, the multiplicity of superimposed regularly structured wall layers of a number of spirilla made the Miller system inappropriate and confusing because of diffraction from multiple and different paracrystalline arrays. Therefore, we have adopted a system, described here, which manages to keep the multiple macromolecular array, then the reflections are divided descriptive as the Miller system. The reflections closest to the axial beam are designated as 100 indices. If these reflections describe more than one macromolecular array then the reflections are divided into 100 and 110 indices, each corresponding to a separate array. The reflections which are next closest to the axial beam are then designated as the 200 series, and once again these can be subdivided into 200 and 210 indices depending on the number of arrays described. This process of indexing is continued through the third, fourth, etc., reflections until all relevant reflections have been indexed. This mode of description was used, in fact, without this statement of procedure, in the description of the arrays of *S. putridiconchylium* (3).

RESULTS

The superficial and regularly structured (RS) layers of *S. metamorphum* were very difficult to analyze on the cell surface. The drying process during negative staining or preparatory to direct platinum-carbon replication caused fragmentation of the structure(s) independent of the growth phase. Furthermore, the layers sloughed off as the culture matured. Once separated from the cells, the layers had a great affinity for one another and formed large complexes containing superimposed RS layers, requiring optical diffraction for analysis. For this reason, freeze-fracturing of cells in the early logarithmic phase was the technique of choice to visualize the superficial layers on the cell surface; unfortunately, the resolution of this technique is limited.

Freeze-fracture observations. Noncryogen-protected cells demonstrated preferential cleavage through the superficial layers, whereas glycerol-treated cells fractured preferentially through the cytoplasm and plasma membrane. Freeze-fracturing of unprotected late logarithmic cells when cleaved along the surface demonstrated that only patches of RS remained on the cells (Fig. 1), whereas early logarithmic cells appeared to be completely covered (Fig. 2). These fractures, which exposed the external surface, were identified by the presence of overlying flagella and/or a circumferential eutectic (8), and they revealed a poorly resolved, hexagonal arrangement of disks (Fig. 2 and 3). Occasionally, when the shadow angle and fracture plane was optimal, delicate delta-linkers (10 to 12 nm long) could be seen joining 8- to 9-nm disks with a center-to-center spacing of 18 to 21 nm (hereafter referred to as the outer structured layer [OSL]) (Fig. 6). Two other superficial layers were also detected: a thin, amorphous, outer layer (OL), which partially masked the OSL (Fig. 6), and an underlying backing layer (BL) which was studded with pits (possibly depressions left by the OSL units) and particles (possibly discrete OSL units left after cleavage) (Fig. 3 and 6). It seemed probable that the poor resolution of the OSL seen in Fig. 2 and 3 was due to a masking effect by the OL. Underlying the BL was a typically pitted OM surface (Fig. 1, 4, 6), although patches of a tetragonal pack-

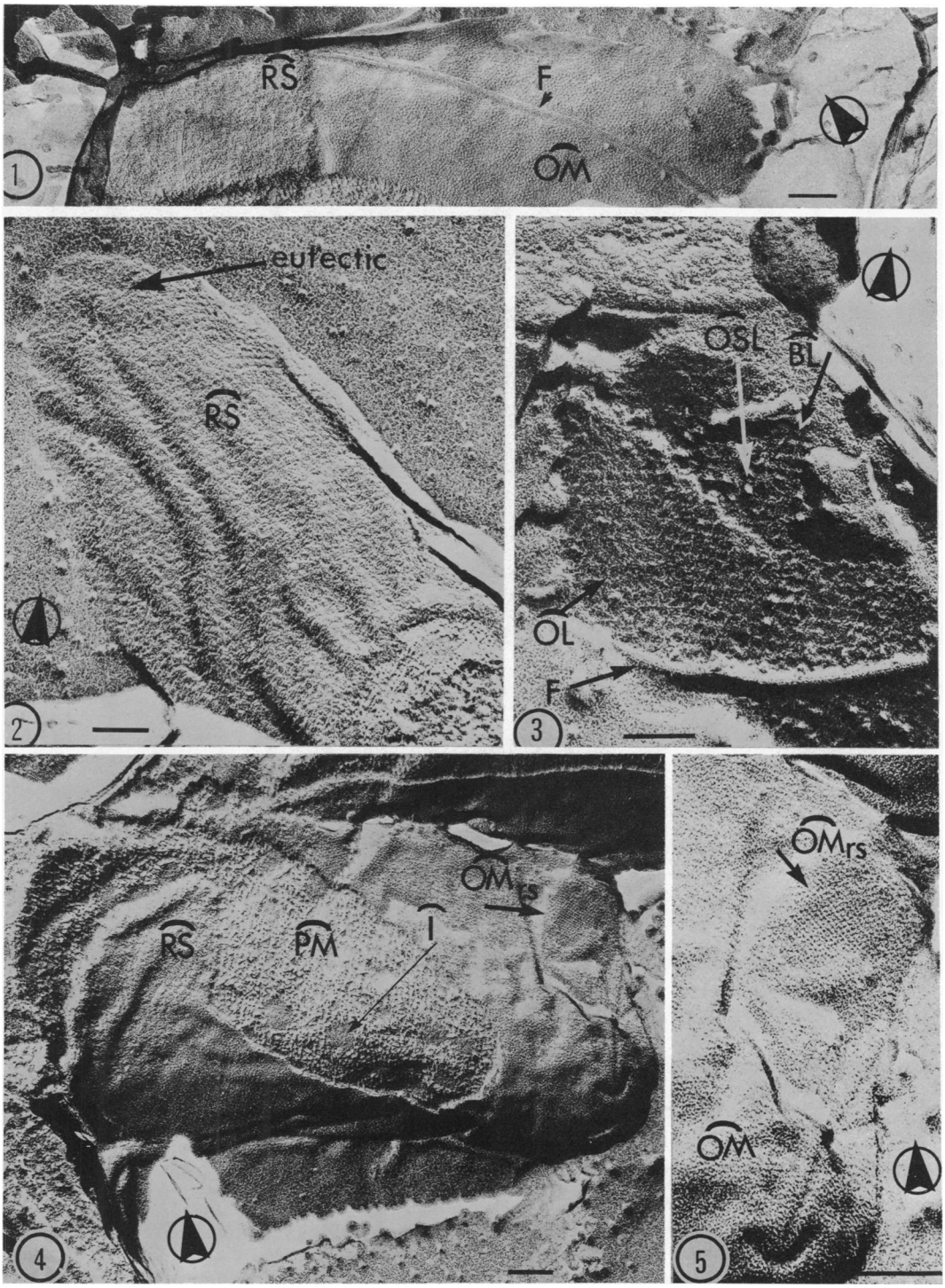

FIG. 1. *Freeze-etched late logarithmic cell of S. metamorphum demonstrating a patch of RS overlying a pitted OM surface. F, Flagellum. All freeze-etchings are nonreversed, the arrow denotes the shadowing direction, and unless otherwise stated the marker indicates 0.1 μm.*

FIG. 2. *Freeze-etched early logarithmic cell demonstrating RS entirely covering the cell surface. Evidence of a peripheral eutectic is seen.*

FIG. 3. *Portion of a freeze-etched early logarithmic cell demonstrating a cleavage through the superficial layers. Particles of an OSL lie intermediate between an OL and a BL. The hexagonal array of the OSL can be seen through the OL surface as well as depressions in the BL surface, which were, presumably, originally occupied by the OSL units before cleavage.*

FIG. 4. *Freeze-etched portion of late logarithmic cell showing an RS fragment, the hydrophobic region of the plasma membrane (PM) with islands (I) devoid of particles, and a tetragonal array (OM_{rs}) on the OM surface.*

FIG. 5. *Higher magnification of OM_{rs} seen in Fig. 4.*

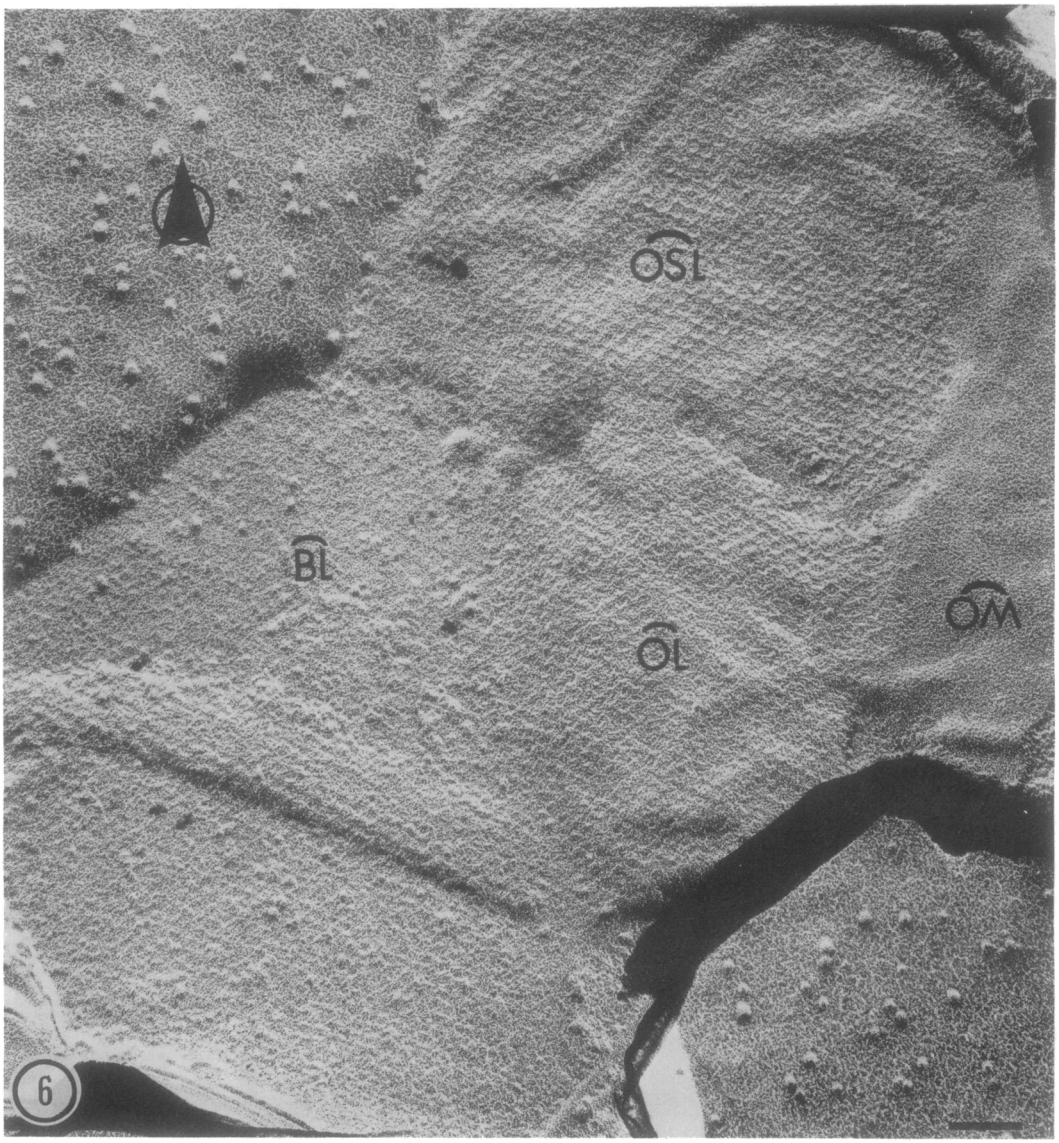

FIG. 6. *Portion of a freeze-etched early logarithmic cell demonstrating the three superficial layers. Careful analysis of the OSL reveals delta-linkers connecting the 8-nm units with center-to-center spacing of 18 to 21 nm.*

ing of small units were occasionally seen (Fig. 4, 5).

Thin sections of whole cells. The superficial layers of *S. metamorphum* were more difficult to visualize in section than was the case for other spirilla studied in our laboratory (3, 5, 14). The usual fixatives (i.e., Ryter-Kellenberger, glutaraldehyde, acrolein, and glutaraldehyde-acrolein) and embedding media (i.e., Vestopal W, Epon 812, and araldite) produced cells completely devoid of superficial wall structure. The addition of ruthenium red to both glutaraldehyde-acrolein fixative and OsO_4 postfixative solutions and the maintenance of suitable Ca^{2+} concentration, as well as the use of water-soluble Durcupan (3), helped retain these layers, but only as an amorphous precipitate. Fortunately, the addition of 2% tannic acid to the glutaraldehyde-acrolein-ruthenium red fixing solution preserved the structural integrity of the superficial structures even though these layers often fragmented off the cells and joined one another to form complex RS structures (Fig. 7, 8, and 9). It appeared that two sets of OL and OSL were

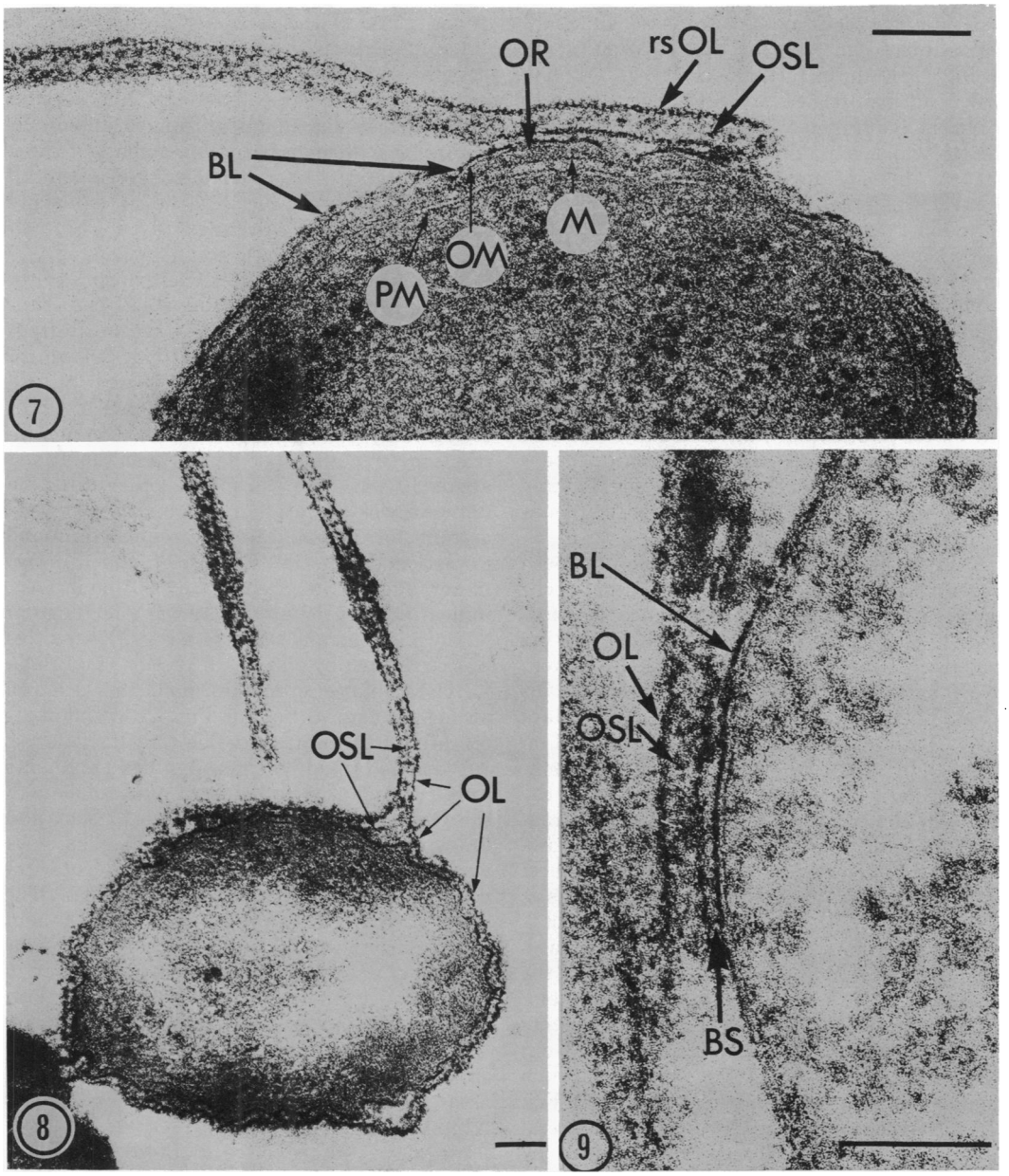

FIG. 7. *Thin section of a portion of a cell which reveals the plasma membrane (PM), mucopeptide (M), OM, an unusually electron-opaque region (OR) between M and OM, and a distinct electron-dense monolayer above OM which is presumed to be the BL. A reassembled piece of RS has readhered to BL and shows a periodicity of 3-nm units (rsOL) in the OL.*

FIG. 8. *Cross-section of a cell undergoing the reassembly process. Two sets of OSL and two sets of OL appear to be involved.*

FIG. 9. *High magnification of a thin section of a reassembled form which has readhered to the BL by means of fibrils of a bridging substance (BS).*

the components involved (Fig. 8), since a thin electron-dense layer (BL) remained on the OM surface (Fig. 7 and 9). The best interpretation of this process appeared to be that the free OSL ends of a single band of OL-OSL would somehow adhere to the free OSL of another OL-OSL band, thus forming an OL-enclosed sandwich of the apposed (i.e., doubled) OSL structures (Fig.

8). The poor resolution of thin sections made it impossible to analyze the intercalation of opposing OSL units further. Once the OL and OSL had reannealed into a stable, cell-free complex, the fragment often adhered back onto the BL which remained above the OM surface; but in this instance the junction occurred between the OL and BL components (Fig. 7 and 9). In most cases small electron-opaque fibrils of a bridging substance could be seen forming this junction (see BS, Fig. 9).

The OL of the fragments exhibited an RS of small 2- to 3-nm units which had not been detected by the freeze-fracture technique of whole cells (see rsOL, Fig. 7). As with the Ordal strain (T. Beveridge and R.G.E. Murray, submitted for publication), an unusually wide and electron-opaque space separated the mucopeptide and OM components (Fig. 7), presumably indicating an abundance of proteinaceous material in this region (1, 16).

Study of superficial layer fragments. Both freeze-fracturing and thin-sectioning techniques have suggested the presence of three discrete superficial layers: a thin BL overlying the OM, an intermediate layer of delta-linked, hexagonally arrayed disks, and an outermost OL of small repeating units (thin-section data only). These layers could not be visualized on the cell by negative staining since this technique caused disruption and reassembly of the released components into complex RS fragments exhibiting superimposition of structure (Fig. 10 and 11). Rotation of Fig. 10 at eye level revealed a major threefold alignment of units at 0°, 60°, and 120°, which was indicative of a hexagonal packing. Minor alignments were also seen at 30°, 150°, and 270°, suggesting the possibility of an underlying hexagonal system. High magnification of one of these fragments demonstrated two distinct components, 8-nm OSL disks (see dOSL, Fig. 11) and much smaller (ca. 3 nm) OL particles (see rsOL, Fig. 11). These small particles, of 10-nm lateral periodicity, were easily seen when aligned by eye along the 0° axis (Fig. 11), and this demonstrated a close association with the disk units.

Fixation and sectioning of these fragments required the same procedures used for whole cells (e.g., compare Fig. 13 with Fig. 14 to 19). Cross-sections confirmed that the fragments were two-sided assemblies composed of two sets of both OSL and OL components, with the OSL units interdigitated with one another in the middle region. The close center-to-center spacing of OL units (ca. 3 nm) seen previously in Fig. 7 was only occasionally seen (Fig. 18), suggesting that the alignment of the fragment to the plane of the section was important. A different periodicity of the OL was also occasionally seen (Fig. 14 and 17), and in this instance the OL appeared to be composed of 10-nm saucer-shaped units. Tangential sections of this layer demonstrated alignments of these small units at a lateral frequency of about 10 nm (see large arrow, Fig. 16); the larger, deeply stained units were presumed to be OSL elements.

Stationary cultures of *S. metamorphum* revealed RS fragments in various states of disruption (Fig. 12, 20, and 22). Occasional fragments of OL alone were seen (Fig. 20) which, when negatively stained and viewed at eye level, revealed two major alignments of small tetragonally arranged units. Viewed in one direaction (0°), the spacing between units was about 10 nm, whereas in the other direction (90°) it was about 5 nm. This appeared to account for the two different frequencies found in sectioned material (Fig. 14, 17, and 18). Two minor alignments occurred at 60° and 120°, indicating that the unit array was a rectangular (10 by 5 nm) arrangement (see Fig. 20), and this was confirmed by optical diffraction (Fig. 20A). A diagrammatic representation of this is shown at high magnification in Fig. 21 without attempting to accurately define the OL units.

When reformed, the reassembled fragments were two-sided, interdigitated assemblies with the OSL units of each lying back to back and breaking the delta-linkers, in which case we would expect a new OSL array with a center-to-center spacing of half of the original. The observed frequencies ranged from 10 to 20 nm, suggesting that the original center-to-center spacing of a single OSL layer would be about 20 nm. Those areas in the fragments which exhibited 10-nm spacing would then be areas where OSL units have interdigitated (labeled I in Fig. 14 and 18), whereas those of 20 nm would be areas where this process did not occur (labeled NI in Fig. 14 and 18).

Negative stains of disrupted stationary growth phase fragments occasionally revealed a single layer of OSL disks (Fig. 12), and it was noted that the center-to-center spacing was 20 nm. In this instance only traces of a linking system could be seen, giving the disks a stellate appearance, and this could be the result of previous interdigitation of OSL units. More often, "naked" OSL fragments (i.e., fragments devoid of OL) were seen with a spacing of 10 nm (Fig. 22), and once again discrete delta-linkers were absent. A higher magnification of these units showed broken linkers pointing between opposing disks (Fig. 23), thereby suggesting

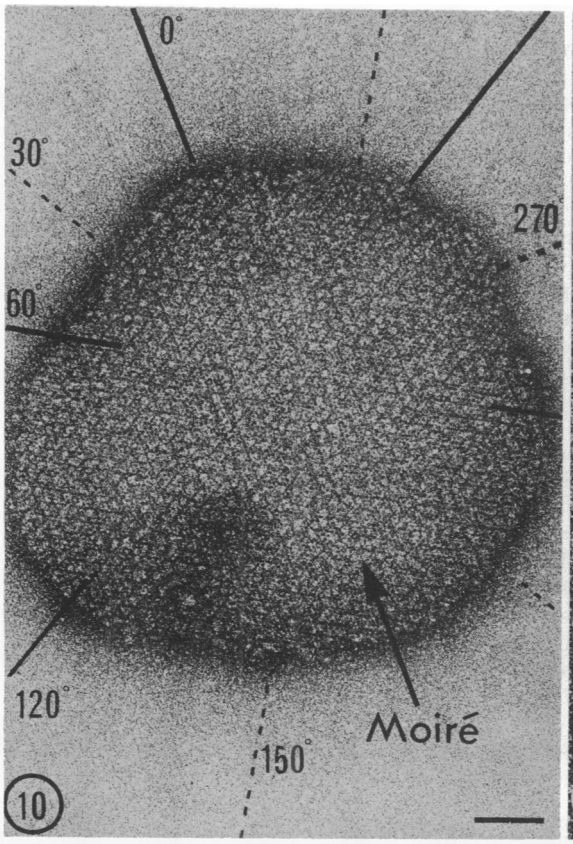

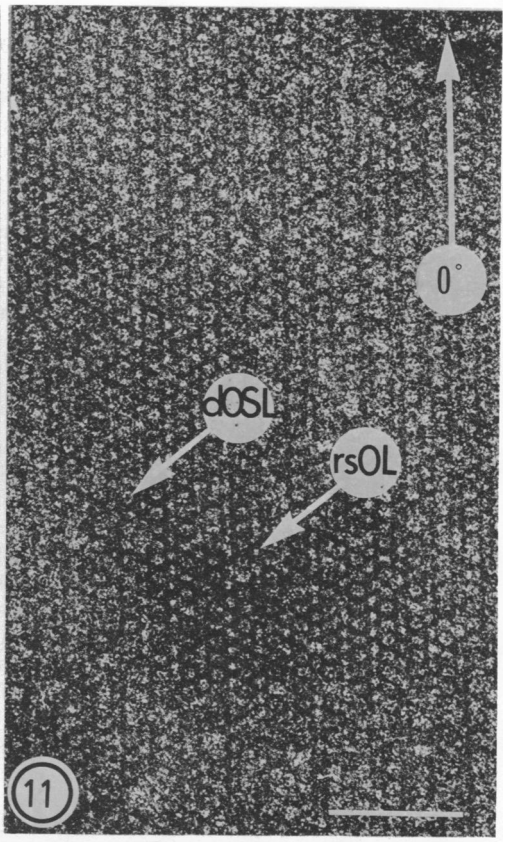

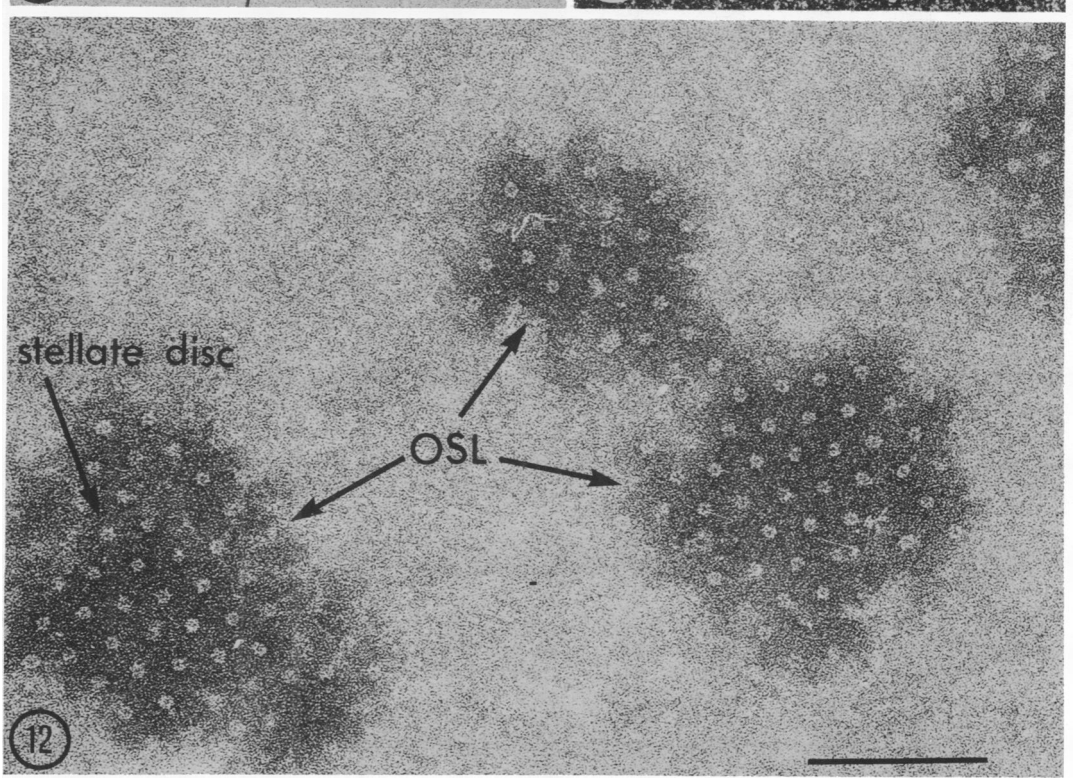

FIGS. 10–12

Y-shaped linkers similar to *S. serpens* strain VHA (5, 14). Freeze-fractured preparations confirmed that these were actually delta-linkers while on the cell surface (Fig. 6) and suggested that these fragments were actually an intercalation of two sets of delta-linked OSL units.

Optical diffraction of OL-OSL fragments. Fragments, such as that seen in Fig. 10, produced the complex transform seen in Fig. 24 when optically diffracted. Diffractometric analysis of this transform revealed two sets of hexagonally arrayed units; one which was described by indices, 110, $\bar{1}10$ $1\bar{1}0$, $\bar{1}\bar{1}0$, $1\bar{1}0$, and $11\bar{0}$, and another described by 111, $11\bar{1}$, $\bar{1}11$, $\bar{1}\bar{1}1$, $1\bar{1}1$, and $1\bar{1}\bar{1}$. Corresponding third-order reflections which describe the finer detail of the OSL units were also seen: indices 330, $33\bar{0}$, $\bar{3}30$, $\bar{3}\bar{3}0$, $3\bar{3}0$, and $3\bar{3}0$ corresponding to the 110 reflections and 333, $\bar{3}33$, $\bar{3}3\bar{3}$, $\bar{3}\bar{3}3$, $3\bar{3}3$, and $33\bar{3}$ to the 111 reflections. Reconstruction utilizing all of these first- and third-order reflections demonstrated the intercalation of OSL units (Fig. 25) which could be separated by blocking-out one set of reflections (Fig. 26) and then the other (Fig. 27). It was of interest to note that some remnants of a delta-linking system could be reconstructed using only these first- and third-order reflections.

The second-order reflections ($\bar{2}20$ and $2\bar{2}0$, and 222 and $\bar{2}\bar{2}2$) appeared to describe the upper and lower (i.e., that lying on the grid surface) 10-nm spacing aspect of the OL, and it was of interest to note that these two layers were arranged at right angles to one another (Fig. 24). Only the upper OL reflected observable points which described its 5-nm periodicity (indices 660 and $\bar{6}60$), and it was apparent that the unit array of the upper OL was a simple, wide, rectangular packing of units described by indices $\bar{2}20$, $\bar{6}60$, $2\bar{2}0$, and 660 (Fig. 24). This was verified by reconstruction of image.

Interpretation of data. Since the drying process during negative staining disrupted the RS layers, there was a major difficulty in visualizing intact superficial layers on cells by high resolution techniques. Only freeze-etched preparations of early and mid-logarithmic cells demonstrated intact surface RS, and the granularity of the shadowing substance made fine resolution impossible. As a result, analyses of negative stains of reassembled fragments were necessary, and this was made difficult by the complexity of the reassemblies. The best interpretation of the data suggested that these reassembled structures consisted of two layers of a regularly structured OL between which rested two sets of intercalated OSL components. An attempt to illustrate this in a diagrammatical way can be seen in the model of a cross-section (Fig. 28). No attempt has been made to accurately define subunit profiles other than that normally resolvable by the thin-sectioning technique; the OSL units have been drawn to resemble a capital "V" and the array of the OL units as small spheres continuous with and attached to the underside of a thin amorphous sheet. The positioning of the OL particle on the underside of the OL sheet is based on the fact that views of freeze-etched OL surfaces were devoid of the loose rectangular array (see Fig. 2, 3, 6). The OL sheet has been drawn as if the section has been cut at right angles to the 10-nm spacing aspect of the OL units. Our interpretation of the original appearance of these layers on the cell surface with respect to the other envelope components may be seen in Fig. 29 and this is based primarily on freeze-fracture (see Fig. 1 to 4 and 6) and thin-section evidence (see Fig. 7 and 8). The original appearance of these layers on the cell surface appeared to be a single OL overlying a single OSL which was loosely connected to a featureless BL (see Fig. 29). The positioning of the OL with respect to the OSL is based upon the data obtained from the study of the reassembled RS forms.

A possible mechanism for the reassembly process has been attempted in Fig. 30. This mechanism is based upon thin-section data of RS layers in the reassembly process (Fig. 8) and the eventual reassembled product (i.e., the alignment of RS units after reassembly has taken place) (Fig. 10, 11, 14, and 16 to 19). As can be seen from this diagrammatical model, we do not believe that BL detaches from the OM and as a result does not contribute structure to the reassembled product.

Many cells demonstrated readherence of the reassembled forms to the BL which had remained on the OM (Fig. 7). High magnification

FIG. 10. *All fragments are stained with ammonium molybdate. Reassembled RS showing moiré of superimposed structure and two threefold sets of alignment.*

FIG. 11. *High magnification of a piece similar to the one seen in Fig. 10. Small (ca. 3 nm) units of the OL (rsOL) show a 5-nm periodicity aligned along the 0° axis. The periodicity of these units is 10 nm when viewed at right angles to the 0° axis. Disks of the OSL (dOSL) may be seen between the rows of rsOL.*

FIG. 12. *Naked OSL fragments found in the supernatant of a stationary phase culture. The OSL units have a stellate appearance and the center-to-center spacing of 20 nm.*

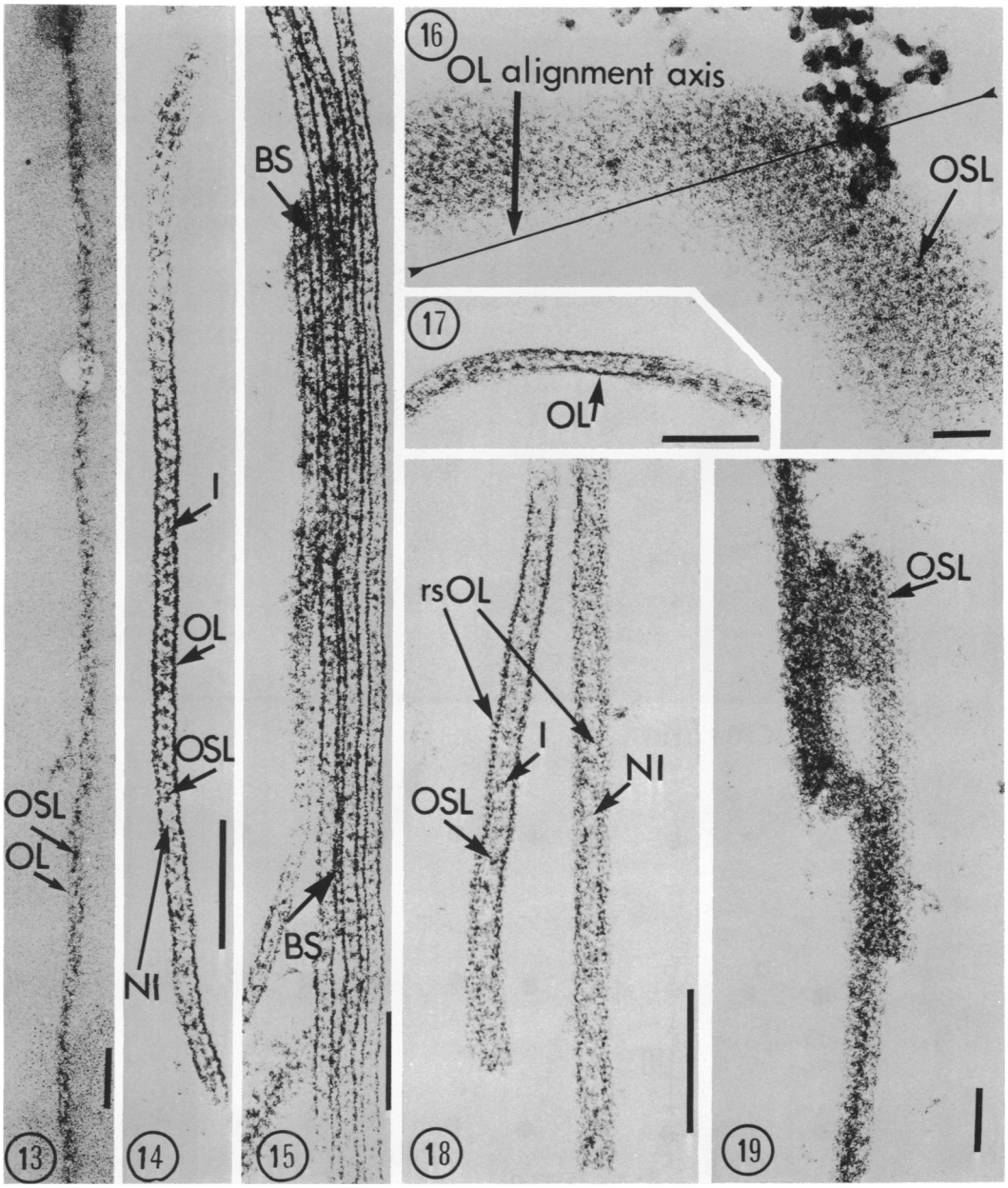

FIG. 13. *Cross-section of a reassembled form which was fixed by glutaraldehyde-acrolein, postfixed with OsO_4, dehydrated through increasing acetone concentrations, and embedded in Vestopal W. Note the poor preservation of structure.*

FIG. 14. *Cross-section of a reassembled form demonstrating a 10-nm periodicity of saucer-shaped units in both sets of OL and a variable periodicity of 8-nm units in the OSL region. The 10-nm spacing of the OSL could be the result of an interdigitation of two sets of OSL units (I), whereas the 20-nm spacing, a result of non-interdigitation (NI).*

FIG. 15. *Thin section of four reassembled forms which are held together by a bridging substance (BS).*

FIG. 16. *Tangential section of a reassembled form showing the OL alignment axis. A 5-nm periodicity of units may be seen running along it and a 10-nm periodicity at right angles to it.*

FIG. 17. *Cross-section of a reassembled form showing the 10-nm spacing aspects of the saucer-shaped units of the OL.*

FIG. 18. *Cross-section of two reassembled forms demonstrating the fine 5-nm spacing of the OL. Interdigitated (I) and non-interdigitated (NI) regions of the OSL are also seen.*

FIG. 19. *Tangential section of a reassembled form showing a hexagonal array of interdigitated OSL units, center-to-center spacing = 10 nm. The reassembled forms in Fig. 14 to 19 were fixed by tannic acid-glutaraldehyde-acrolein-ruthenium red, postfixed with OsO_4, and embedded in water-soluble Durcupan.*

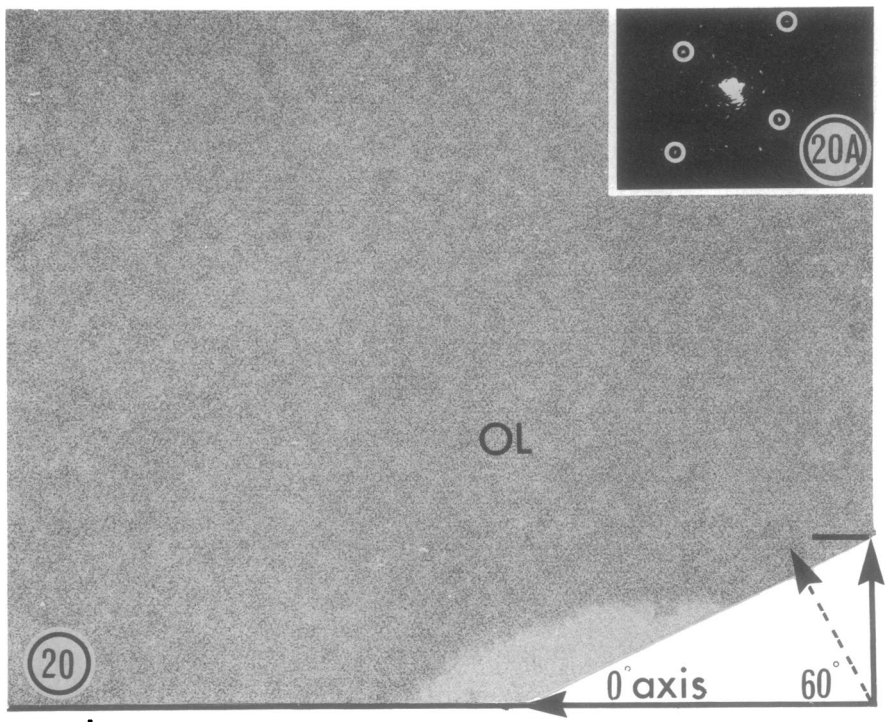

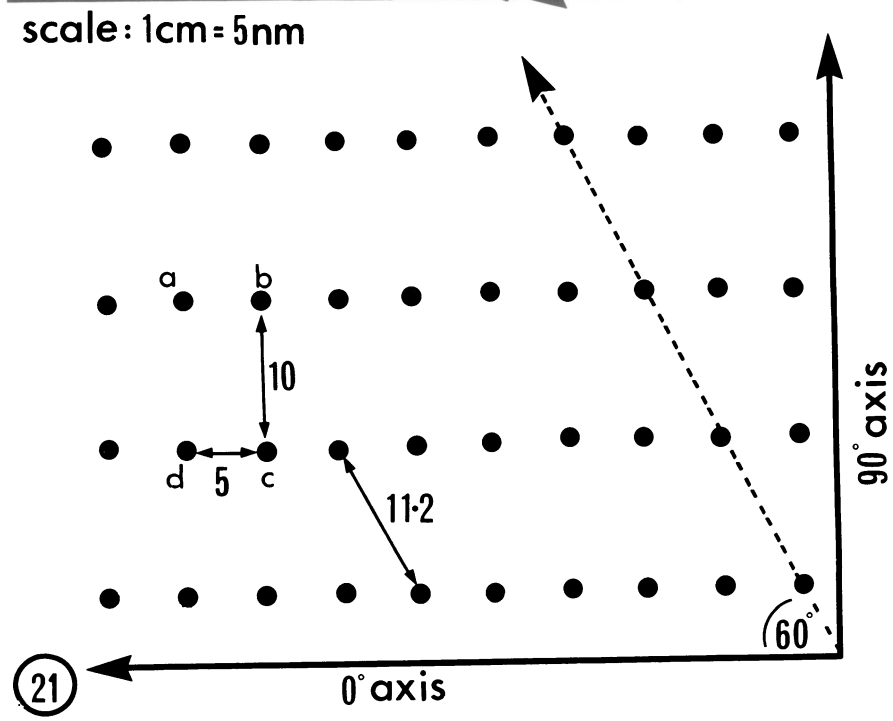

FIG. 20. *Ammonium molybdate-stained OL fragment from a stationary phase culture of cells on which two major alignments (0° and 90°) and one of the minor alignments (60°) have been drawn. These alignments are indicative of a loose rectangularly packed array. The bar = 0.1 μm. (A) Optical transform of the fragment in Fig. 20. No attempt has been made to align the transform with the fragment.*

FIG. 21. *Diagrammatical model of the arrangement of OL units. No attempt has been made to accurately define these units other than small spheres. The four units outlined by a, b, c, and d describe the unit cell. The distances are in nanometers.*

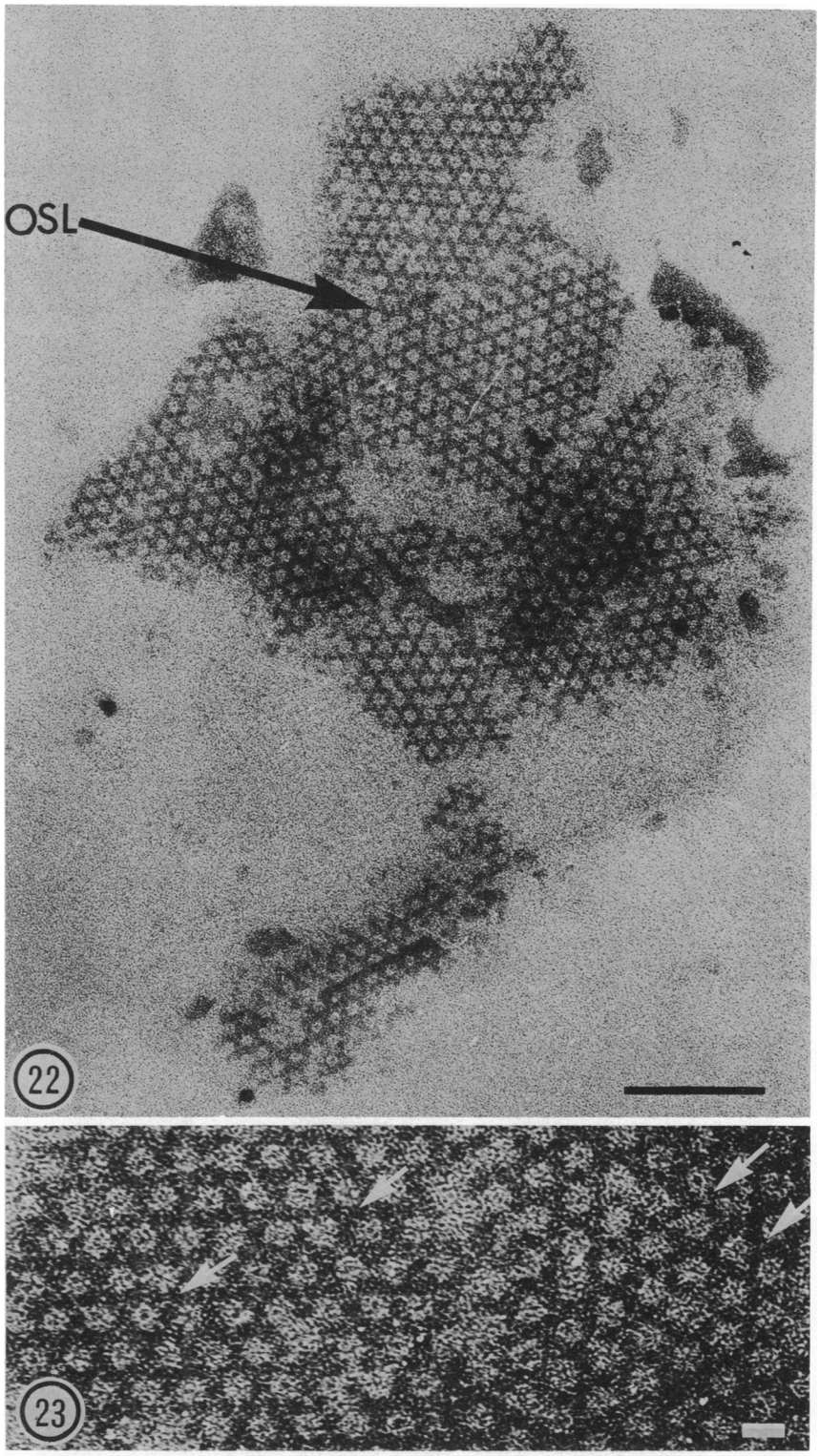

FIG. 22. *Phosphotungstic acid-stained OSL fragment from a stationary phase culture of cells which exhibits a 10-nm periodicity of hexagonally arranged OSL units. The bar = 0.1 μm.*

FIG. 23. *High magnification of Fig. 22. Arrows indicate remnants of linkers which point between adjacent OSL units. The bar = 10 nm.*

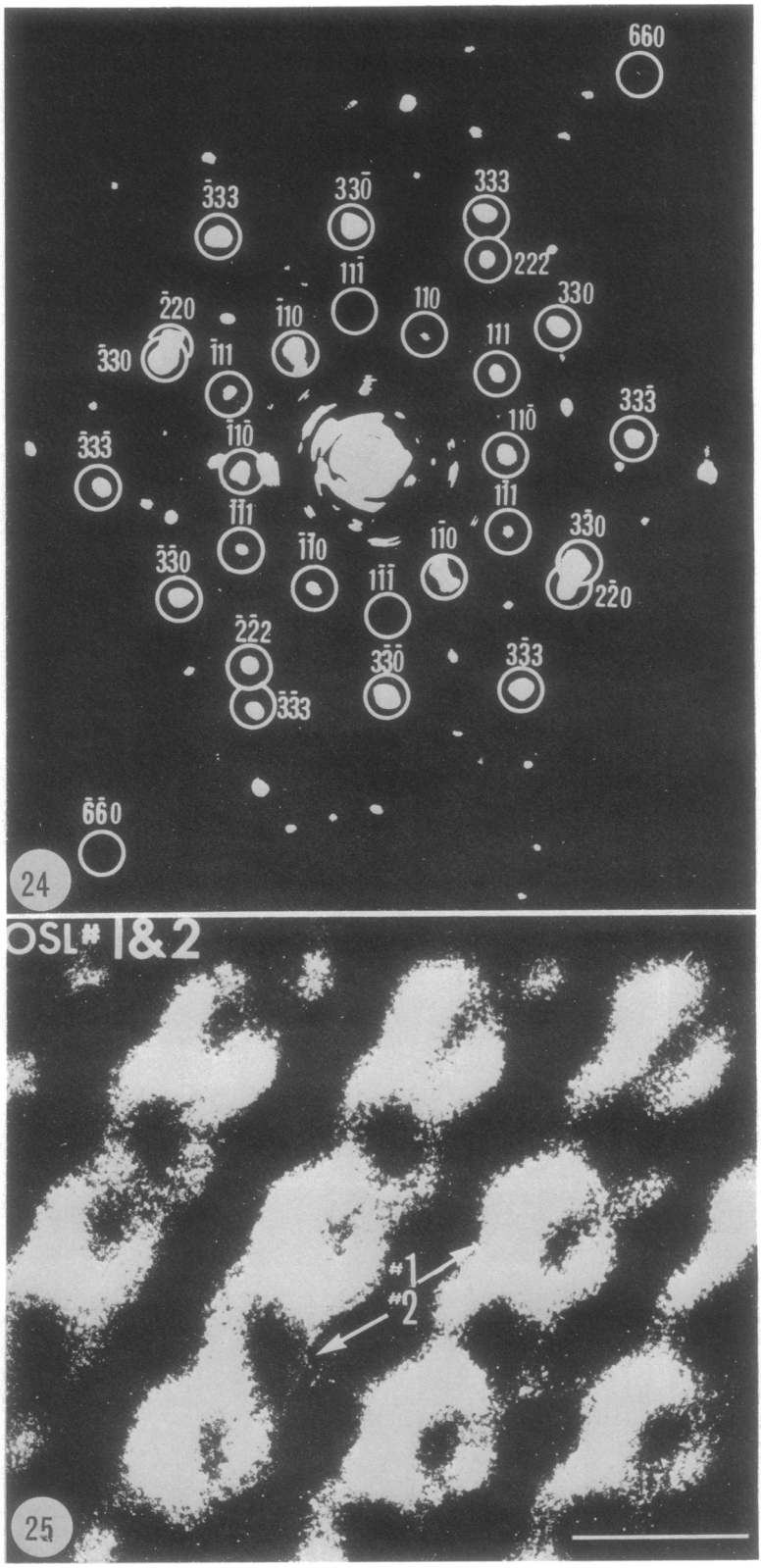

FIG. 24. *Optical transform derived from a negatively stained RS fragment similar to that seen in Fig. 10. See text for indexing system.*

FIG. 25. *Reconstruction of image utilizing all first- and third-order reflections in Fig. 24. Both the upper (#1) and lower (#2) OSL sets are seen. Diameter of OSL units is 8 nm.*

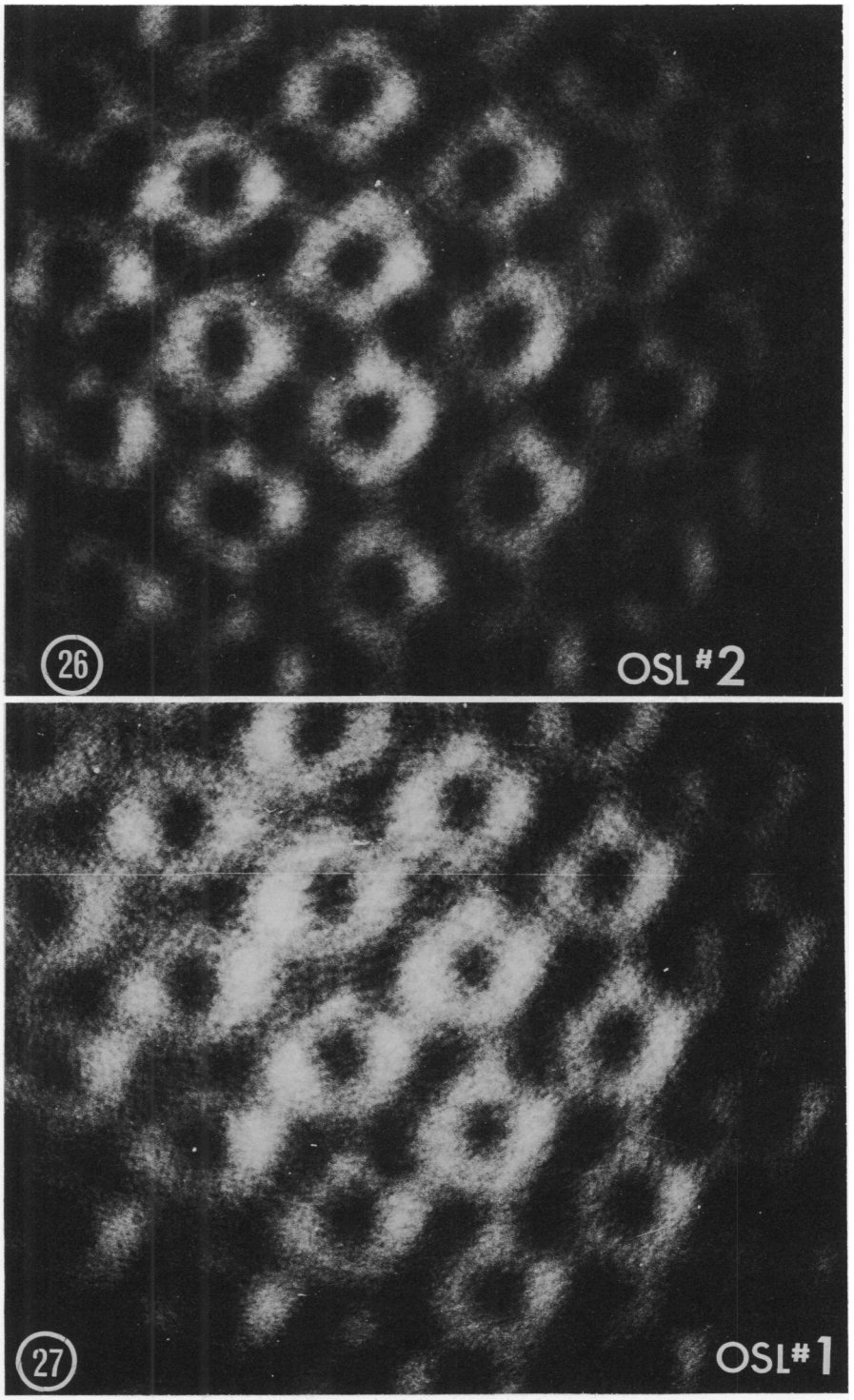

FIG. 26. *Reconstruction of image utilizing reflections 111 → $1\bar{1}1$ and 333 → $33\bar{3}$ of optical transform seen in Fig. 24. The OSL disks are connected by remnants of delta-linkers. OSL #2 = lower OSL set.*

FIG. 27. *Reconstruction of image utilizing reflections 100 → $11\bar{0}$ and 330 → $3\bar{3}0$. Once again remnants of delta-linkers are seen. OSL #1 = upper OSL set.*

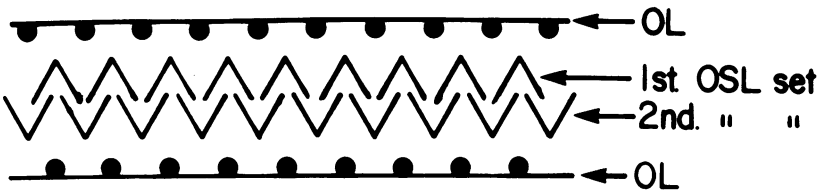

Fig. 28

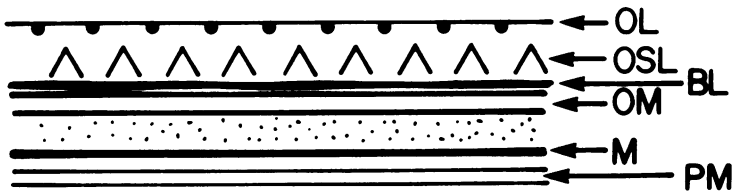

Fig. 29

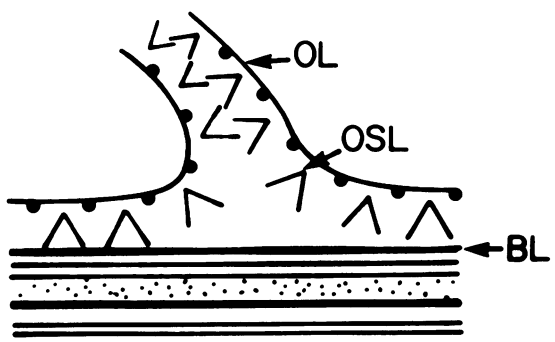

Fig. 30

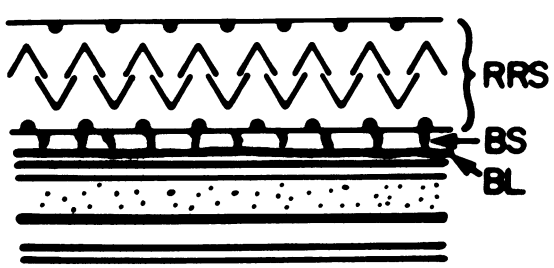

Fig. 31

FIG. 28. *Diagrammatical model of a reassembled RS fragment from S. metamorphum . No attempt has been made to accurately define the shape of the units although OSL and OL alignment fits optical diffraction data.*

FIG. 29. *Diagrammatical model of the arrangement of the superficial layers on the cell surface.*

FIG. 30. *Diagrammatical model of the reassembly process during the formation of the RS fragments.*

FIG. 31. *Diagrammatical model of a reassembled RS fragment (RRS) which has adhered to the BL of the cell surface by the bridging substance (BS).*

of thin sections of these cells revealed the junction of the reattachment to be caused by amorphous fibrils of a bridging substance (Fig. 9) and this has been diagrammatically illustrated in Fig. 31.

DISCUSSION

"Any kind of a repeat organization is a crystal in a [generalized crystallographic] sense" (2). Several spirilla exhibit close-packed, hexagonal arrays of macromolecules on the external surface of their cell walls, and *S. serpens* strain VHA is a prime example (5, 14). The spirillum used in this study (*S. metamorphum*) differs from *S. serpens* strain VHA in the number of superficial layers and in the diversity of macromolecular arrangement of the RS components. *S. metamorphum* contains three distinct superficial layers, one of which (the OL) contains a loose rectangular packing of units, another (the OSL) consists of a delta-linked, hexagonal array, and, finally, an amorphous BL which sits immediately adjacent to a pitted OM surface. *S. serpens* strain VHA, on the other hand, contained one distinct superficial layer and this was composed of a Y-linked, hexagonal array (5, 14). Both of these spirilla and *S. putridiconchylium* contained an OM surface which was pitted (in the case of *S. putridiconchylium*, this was often in a regular, hexagonal manner [3]), and this conforms well with the OMs of other spirilla which have been studied in our laboratory (3, 5; T. Beveridge and R. G. E. Murray, unpublished results).

The superficial layers of *S. metamorphum* were unusual in that two of the component parts (the OL and OSL) appeared to be loosely adherent to the remainder of the cell wall and fragmented off the surface to interact and form complex RS structures with one another. This was especially true with late logarithmic and stationary cultures and could not be inhibited by the addition of calcium which has previously been shown to have a stabilizing influence on spirillum RS (3, 5, 6). As with the RS layers of *S. putridiconchylium*, the superficial layers of *S. metamorphum* proved unusually sensitive to organic solvents, such as ethanol and acetone, and for this reason ordinary dehydration and embedding (i.e., Epon 812, Vestopal W, etc.) procedures could not be used in the preparation of sectioned material.

Preservation of structure in sections required an elaborate fixation procedure involving ruthenium red as a cationic stabilizing agent (3), aldehydes as cross-linking agents for proteins (10, 12), and tannic acid as an additional linking agent. Tannic acid is a glucoside which consists of several reactive orthopolyphenol groups which allow it to precipitate proteins, polypeptides, alkaloids, and metallic cations (9, 13). The reactivity of tannic acid with proteins has been calculated to be approximately 1,000 times that of the aldehyde group of fixatives (13), and the constituent orthopolyphenol groups may combine with the protein by forming either hydrogen or chelate bonds (9). In fact, in the specific case of *S. metamorphum* superficial layers, it may have at least two functions: the tannic acid may strongly cross-link the RS macromolecules (which are proteinaceous; T. Beveridge, unpublished results), perhaps in their native configurations, as well as forming complexes with the RS-stabilizing ruthenium red cations, thereby increasing the electron density of the layers. Unfortunately, this fixation procedure was unable to irreversibly bind the OSL-OL complex to the BL of the cell surface, and the manner in which these layers reassembled with one another to form complex forms with superimposed structure suggests that some reactive groups remained unlinked.

Bacterial extracellular proteins often have a deficiency of sulfur-containing amino acids and, therefore, disulfide bonds are absent or infrequent (15). These bonds are the most important, if not the only, covalent linkages contributing to the stability and rigidity of the tertiary structure of protein molecules (4), and their absence would have to be replaced by hydrogen bonds and metal- and salt-linkages which are not nearly as strong (15). A lack of disulfide linkages has already been demonstrated in the hexagonal array of macromolecules on the cell surface of *S. serpens* strain VHA (6) and this may be true of most superficial layers on spirilla. Electron microscopy indicates that the reassembled OSL-OL forms of *S. metamorphum* resist the action of both dithiothreitol and β-mercaptoethanol (T. Beveridge, unpublished results), which should break disulfide bonds if these linkages were available to the agents. Unfortunately, an amino acid analysis of these layers on *S. metamorphum* has not been performed, but it is attractive to hypothesize that their easy disruption may stem from a low cyst(e)ine content.

ACKNOWLEDGMENTS

We are grateful to M. Hall, J. Marak, and G. Sanders for expert technical assistance during this project. We wish to thank N. R. Kreig (Department of Biology, Virginia Polytechnic Inst., Blacksburg, Virginia) and P. B. Hylemon (now at Virginia Commonwealth University, Richmond, Virginia) for supplying us with cultures and information about them.

The financial support of the Medical Research Council of Canada is gratefully acknowledged.

LITERATURE CITED

1. Beer, M. 1965. Selective staining for electron microscopy. Lab. Invest. **14**:1020–1025.
2. Bernal, J. D. 1966. Opening remarks of principles of biomolecular organization, p. 3. *In* G. E. W. Wolstenholme and M. O'Connor (ed.), Ciba Foundation symposium. J. & A. Churchill Ltd., London.
3. Beveridge, T. J., and R. G. E. Murray. 1974. Superficial macromolecular arrays on the cell wall of *Spirillum putridiconchylium*. J. Bacteriol. **119**:1019–1038.
4. Boyer, P. D. 1959. Sulfhydryl and disulfide groups of enzymes, p. 454–588. *In* P. D. Boyer, H. Lardy, and K. Myrbäck (ed.), The enzymes, vol. 1, 2nd ed. Academic Press, Inc., New York.
5. Buckmire, F. L. A., and R. G. E. Murray. 1970. Studies on the cell wall of *Spirillum serpens*. I. Isolation and partial purification of the outermost cell wall layer. Can. J. Microbiol. **16**:1011–1022.
6. Buckmire, F. L. A., and R. G. E. Murray. 1973. Studies on the cell wall of *Spirillum serpens*. II. Chemical characterization of the outer structured layer. Can. J. Microbiol. **19**:50–66.
7. Cox, R. W., and R. W. Horne. 1968. Accurate calibration of the A.E.I. E.M. 6B/2 electron microscope using catalase crystals, p. 579–580. *In* Fourth European Regional Conference on Electron Microscopy. Tipographia Poliglotta Vaticana, Rome.
8. DeVoe, I. W., J. W. Costerton, and R. A. MacLeod. 1971. Demonstration by freeze-etching of a single cleavage plane in the cell wall of a gram-negative bacterium. J. Bacteriol. **106**:659–671.
9. Futaesuka, Y., V. Mizuhira, and H. Nakamura. 1972. The new fixation method using tannic acid for electron microscopy and some observations of biological specimens, p. 155–156. *In* Proc. 4th Int. Congr. Histochem. Cytochem., Kyoto, Japan.
10. Hayat, M. A. 1970. Principles and techniques of electron microscopy: biological applications, vol. 1. Van Nostrand Reinhold Co., New York.
11. Hylemon, P. B., J. S. Wells, Jr., N. R. Krieg, and H. W. Jannasch. 1973. The genus *Spirullum*: a taxonomic study. Int. J. Syst. Bacteriol. **23**:340–380.
12. Korn, A. H., S. H. Feairheller, and E. M. Filachoine. 1972. Glutaraldehyde: nature of the reagent. J. Mol. Biol. **65**:525–529.
13. Mizuhira, V., and Y. Futaesaku. 1972. New fixation for biological membranes using tannic acids. Acta Histochem. Cytochem. **5**:233–235.
14. Murray, R. G. E. 1963. On the cell wall structure of *Spirillum serpens*. Can. J. Microbiol. **9**:381–391.
15. Pollack, M. R., and M. H. Richmond. 1962. Low cyst(e)ine content of bacterial extracellular proteins: its possible physiological significance. Nature (London) **194**:446–449.
16. Reynolds. E. S. 1963. The use of lead citrate at high pH as an electron-opaque stain in electron microscopy. J. Cell. Biol. **17**:208–212.
17. Taylor, C. A., and H. Lipson. 1964. Optical transforms. G. Bell and Sons, Ltd., London.